

Dielectric evidence of persistence of polar nanoregions within the ferroelectric phases of $(1 - x)\text{Pb}(\text{Zn}_{1/3}\text{Nb}_{2/3})\text{O}_3 - x\text{PbTiO}_3$ relaxor ferroelectric system

Mouhamed Amin Hentati,^{1,2,3} Hichem Dammak,³ Hamadi Khemakhem,² Nicolas Guiblin,³ and Mai Pham Thi⁴

¹Department of Physics, University College in Leith, Umm Al-Qura University, Makkah, Saudi Arabia

²Laboratoire des Matériaux Ferroélectriques, Faculté des Sciences de Sfax, Route Soukra Km 3,5, B.P.802, 3018 Sfax, Tunisia

³Laboratoire Structures, Propriétés et Modélisation des Solides UMR 8580 CNRS, CentraleSupélec, Université Paris-Saclay, 92295 Châtenay-Malabry, France

⁴Laboratoire Nanocomposites & Matériaux Hétérogènes, THALES Research & Technology-France, RD 128, F-91767 Palaiseau cedex, France

(Received 28 April 2015; accepted 5 July 2015; published online 17 July 2015)

The electromechanical and structural properties of [001] and [111]-oriented $\text{Pb}(\text{Zn}_{1/3}\text{Nb}_{2/3})\text{O}_3 - 6\%\text{PbTiO}_3$ (PZN – 6%PT) single crystals have been characterized using dielectric spectroscopy, x-ray diffraction, depolarization current, and piezoelectric techniques from 80 K to 300 K. Both unpoled and poled samples show a dielectric loss peak located in the range from 100 to 200 K. The poled samples show a change in the slope of the real part of the dielectric permittivity and a broad, frequency dependent peak in the imaginary part below 200 K. In the same temperature range, we observed a broadening of the Bragg peaks, fluctuations in the macroscopic polarization, and a change in the rate of decrease in the elastic compliance and the d_{31} piezoelectric coefficient. These results were analyzed within the framework of three models proposed in the literature. This analysis argues that these observations originate from the freezing of the dynamics of the polar nanoregions (PNRs) at low temperature. This assumption implicates two important results; (i) the PNRs are embedded and persist within the ferroelectric, low-temperature phases, and (ii) they contribute to the large piezoelectric properties of the PZN – $x\%$ PT single crystals. These conclusions may be general to all ferroelectric relaxor systems. © 2015 AIP Publishing LLC. [<http://dx.doi.org/10.1063/1.4926877>]

I. INTRODUCTION

Solid solutions of $(1-x)\text{Pb}(\text{Zn}_{1/3}\text{Nb}_{2/3})\text{O}_3 - x\text{PbTiO}_3$ (PZN– $x\%$ PT) and $(1-x)\text{Pb}(\text{Mg}_{1/3}\text{Nb}_{2/3})\text{O}_3 - x\text{PbTiO}_3$ (PMN– $x\%$ PT) are of great interest because of their promising electromechanical properties.^{1,2} For example, PZN– $x\%$ PT, with $0\% \leq x \leq 15\%$, exhibit very large piezoelectric coefficients ($d_{33} \geq 500$ pC/N) and electromechanical coupling factors ($k_{33} \geq 80\%$).^{1,2} From a theoretical point of view, these interesting properties have been attributed essentially to a strong “polarization rotation effect” under electric field.³ Experimentally, Kutnjak and coworkers postulate that the large electromechanical response can be expected whenever a system is close to criticality.⁴ PZN– $x\%$ PT and PMN– $x\%$ PT are also (for small x) prototypical ferroelectric relaxors that exhibit a large and strongly frequency-dependent dielectric permittivity, which peaks broadly in temperature.⁵ These behaviors have been linked to the presence of polar nanoregions (PNRs),⁶ which appear below the Burns temperature T_B .⁷ Extensive neutron and x-ray diffuse scattering studies show that the PNRs persist within the ferroelectric phases.^{8–13} Previous studies suggest a close relationship between PNRs and the ultrahigh piezoelectric response in PZN– $x\%$ PT (Refs. 11 and 14) and PMN– $x\%$ PT (Ref. 15) systems, as well as in the magnetic relaxor Galfenol.¹⁶

In this paper, we present dielectric evidence of the presence of PNRs within the ferroelectric low temperature phases of the PZN– $x\%$ PT system. In addition, we prove that these PNRs contribute to the outstanding piezoelectric properties of this system. Practically, we decided to focus on a specific composition (PZN–6%PT) and to study its dielectric, electromechanical, pyroelectric, and structural properties from 300 K down to 80 K, with and without a bias electric field along the [001] and [111] crystallographic directions.

II. EXPERIMENTAL DETAILS

PZN – $x\%$ PT single crystals were grown using the conventional high temperature flux method described elsewhere.^{17,18} Crystals were oriented, by the Laue backscattering method, along [001] and [111] pseudocubic directions and cut with a wire saw to obtain longitudinal rods with dimensions of $8 \times 1.5 \times 1.5$ mm³ and mass of 0.152 g. Samples were then polished and gold electrodes were sputtered on their relevant faces, after which they were annealed in nitrogen at 500 K for 2 h to release the stress induced by polishing.

Dielectric measurements were performed using Agilent 4294A and HP4192A LF impedance analyzers connected with a computer controlled temperature chamber.

These measurements were made on heating from 80 K to 300 K at a rate of 2 K/min (zero field heating). [001] and [111] oriented crystals were poled by field-cooling from 500 K to 80 K under a constant dc bias of 0.5 kV/cm. The macroscopic polarization P_S was calculated by integration of the pyroelectric current, measured using a Keithley 617 electrometer during a heating of poled samples.

The electromechanical properties of [001]-oriented, poled, single crystal were measured as a function of temperature using the resonance-antiresonance method, following IEEE standards,¹⁹ using an HP 4192 impedance analyzer.

The x-ray diffraction (XRD) patterns were recorded with a high-resolution two-axis diffractometer, using $\text{Cu K}\beta$ ($\lambda = 0.139223$ nm) monochromatic radiation issued from a Rigaku rotating anode (RU300, 18 kW). The powder sample was obtained by grinding single crystals at room temperature. The powder was sieved ($d \leq 50 \mu\text{m}$) and then annealed at 470 K in order to reduce strains induced by grinding. Samples (single crystal or powder) were fixed on a copper holder inside a N_2 flow cryostat (80–470 K) mounted on a HUBER goniometric head. In the Bragg–Brentano geometry, the diffraction angles were measured with a relative precision better than 0.002° (2θ). Two-dimensional maps of the diffracted intensity were also recorded, rotating the crystal step by step around the ω axis. Such $\theta - \omega$ mappings allow us to characterize the domain structure of the crystals and then to determine its symmetry.¹⁷

III. RESULTS AND DISCUSSION

A. Dielectric evidence of the presence of PNRs within the ferroelectric low temperature phases of the PZN– $x\%$ PT system

The thermal evolution of the dielectric permittivity and loss of an unpoled [001]-oriented rod (PZN–6%PT) at various frequencies is given in Fig. 1. The real part (ϵ') of dielectric permittivity (Fig. 1(a)) rises up gradually on heating and an obvious frequency dependence is visible above 80 K. For the imaginary part (ϵ'') of the dielectric permittivity (Fig. 1(a)), a frequency dependent plateau region was observed between 80 and 200 K. At higher temperatures, the response becomes non-dispersive and strongly temperature dependent. As shown in Fig. 1(b), a broad peak in the dielectric loss ($\tan \delta$) can be observed in the same temperature range. With increasing frequency, the maximum in $\tan \delta$ shifts to higher temperatures. This peak is also observed for different crystallographic directions ([110] and [111]) and in other samples with different composition x , such as 0%, 4.5%, 7%, 9%, and 12% (Fig. 1(c)), indicating a reproducible behavior for the PZN– $x\%$ PT system. The inset in Fig. 1(b) shows the measurement frequency as a function of the peak temperature. The data were fitted to the Arrhenius and the Vogel–Fülcher relations, respectively,

$$f = f_0 e^{-E_a/(k_B T_m)},$$

$$f = f_0 e^{-E_a/(k_B(T_m - T_{VF}))},$$

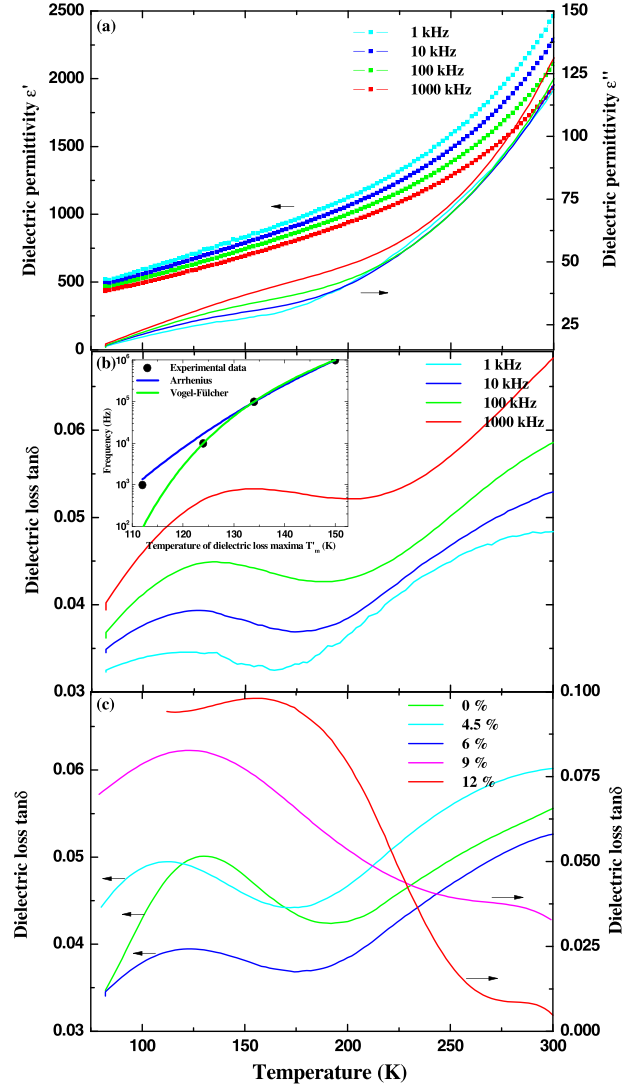


FIG. 1. Temperature dependence of (a) the real and imaginary parts of dielectric permittivity, and (b) the dielectric loss of [001] oriented and unpoled PZN – 6%PT single crystal at various frequencies. Inset shows the measurement frequency as a function of the peak temperature (dots: experimental data; blue curve: fitting to Arrhenius relation; green curve: fitting to Vogel–Fülcher relation). (c) The dielectric loss of [001] oriented and unpoled PZN – $x\%$ PT single crystals with different composition x at 10 kHz.

where f is the measurement frequency, f_0 the pre-exponential term, E_a the activation energy, k_B the Boltzmann's constant, T_m the temperature of maximum dielectric loss, and T_{VF} the Vogel–Fülcher temperature. The fit parameters are $E_a = (0.250 \pm 0.005)$ eV and $f_0 = (2.8 \pm 1.2) 10^{14}$ Hz for the Arrhenius relation and $E_a = (0.046 \pm 0.008)$ eV, $f_0 = (2.2 \pm 1.5) 10^9$ Hz, and $T_{VF} = (80 \pm 5)$ K for the Vogel–Fülcher relation. These results are similar to those obtained on the PZN–4.5%PT (Ref. 20) and PZN–9%PT.²¹

This dielectric anomaly is typical of PZN– $x\%$ PT (Refs. 20–25) and PMN– $x\%$ PT (Refs. 26–31) relaxor ferroelectric systems within the morphotropic phase boundary and on rhombohedral and tetragonal sides of their phase diagrams at low temperature. In the literature, three different models are generally proposed to explain its physical origin. The first

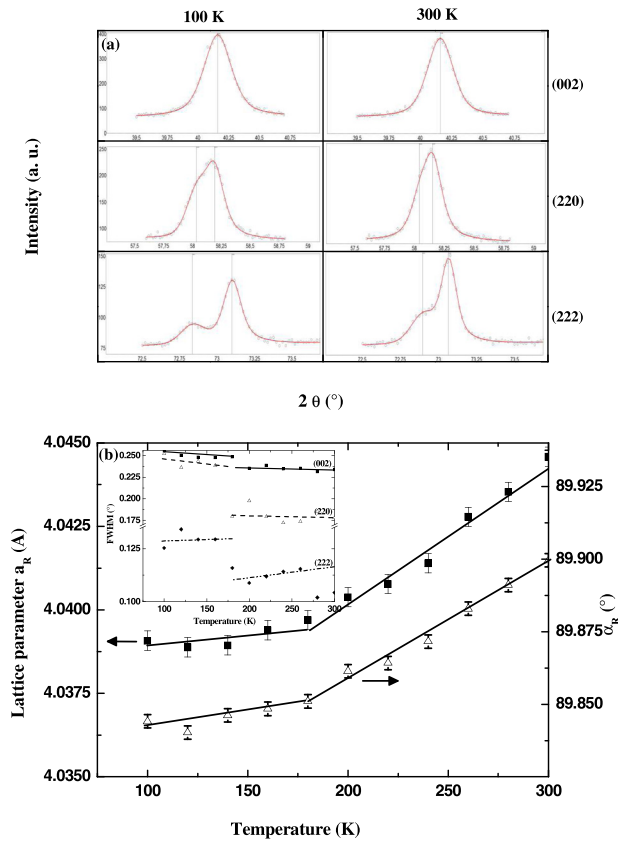


FIG. 2. (a) Diffraction profiles of pseudocubic reflections (002), (220), and (222) for PZN – 6%PT at 300 and 100 K (circles: experimental data; continuous red line: fitting using pseudo-Voigt profile; vertical line: calculated positions of the Bragg reflections). (b) Temperature dependence of the rhombohedral lattice parameters for PZN – 6%PT powder. Inset shows the variation of the full widths at half maximum (FWHM) of the profiles of (002), (220), and (222) Bragg reflections as a function of temperature.

attributes this anomaly to a structural phase transition between two ferroelectric phases.^{24–26} The second suggests that the anomaly in the dielectric loss observed at low temperature is dominated by the motion/relaxation of domain walls.^{20,21,30} The third assumes the existence of structural irregularities (clusters) within the ferroelectric domains that are responsible for relaxation phenomenon.²⁷

In order to determine the origin of this cryogenic dielectric relaxation process, XRD measurements were performed, on a PZN-6%PT powder sample from 300 K to 100 K. We present in Fig. 2(a) the profiles of the (002), (220), and (222) pseudocubic reflections at 100 and 300 K. For these two temperatures, the (002) is a singlet, while (220) and (222) are doublets with weaker reflections occurring on the lower 2θ side, typical of a rhombohedral phase that is stable for temperatures between 300 and 100 K. According to this result, the dielectric anomaly is unlikely to be associated with a long-range structural phase transition, which is in good agreement with the phase diagram previously reported on PZN- x %PT system.^{32,33} Fig. 2(b) and the inset in Fig. 2(b) show the thermal evolution of the extracted cell parameters and the full width at half maximum (FWHM) of the (002), (220), and (222) pseudocubic reflections, respectively. On cooling, the rhombohedral lattice parameters (a_R and α_R) decrease and do so more rapidly below 200 K. Close

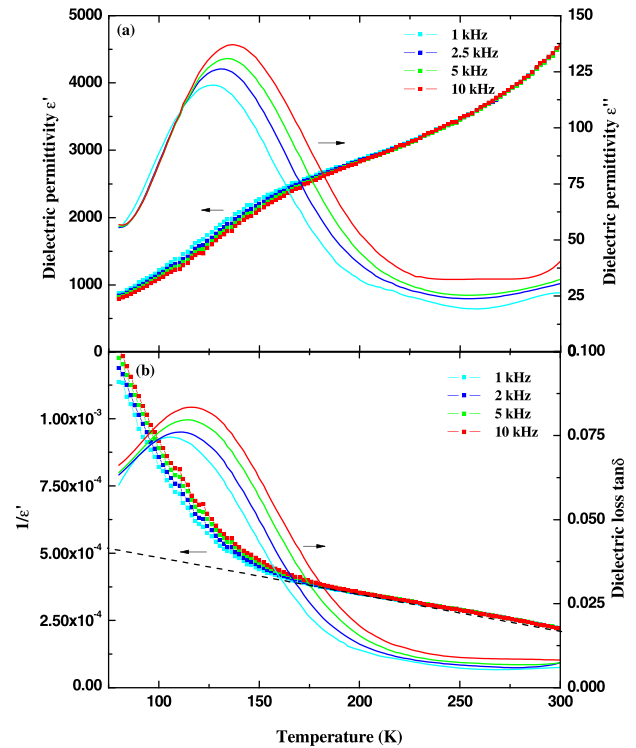


FIG. 3. Temperature dependence of (a) the real and imaginary parts of dielectric permittivity, and (b) the reciprocal of the real part and the dielectric loss of [001] oriented and poled PZN – 6%PT single crystal at various frequencies.

to the same temperature, the different pseudocubic reflections show a sudden broadening, which is probably due to a change in the microstrains within the material. This broadening is also observed in PZN.³⁴

The second model proposed in the literature attributes this low-temperature relaxation to domain wall motions. To test this assumption, we measured the temperature dependence of some dielectric properties for poled [001] and [111] oriented single crystals at different frequencies (the 100 kHz and 1 MHz data are excluded due to the influence of piezoelectric resonance) from 80 to 300 K (Figs. 3 and 4). Indeed, it is well known that poling induces a stable domain structure that explains the absence of domain wall motion in poled samples.¹ Compared with the unpoled sample, the [001] poled sample shows a change in the slope of ϵ' and a frequency dependent broad peak in ϵ'' below 200 K (Fig. 3(a)). Above 200 K, the reciprocal of ϵ' has good linear relationship with temperature (Fig. 3(b)). In the same temperature range, the dielectric loss shows a lower background and less frequency dispersion, which is explained by the decrease of the extrinsic contributions to the dielectric loss, typically from domain wall motion, in the poled samples. A similar behavior was observed in the [110] (not plotted) and [111] (Fig. 4) directions. For the latter direction, the dielectric permittivity ϵ' is the lowest indicating that the polar axis is parallel to [111] axis and the sample is in a rhombohedral single domain state 1R. In order to verify the domain structure of the low temperature phase, $\theta - \omega$ mapping of the [111] poled sample was recorded, at 90 K, around the (222) pseudocubic reflection in the reciprocal plane perpendicular to [110] direction

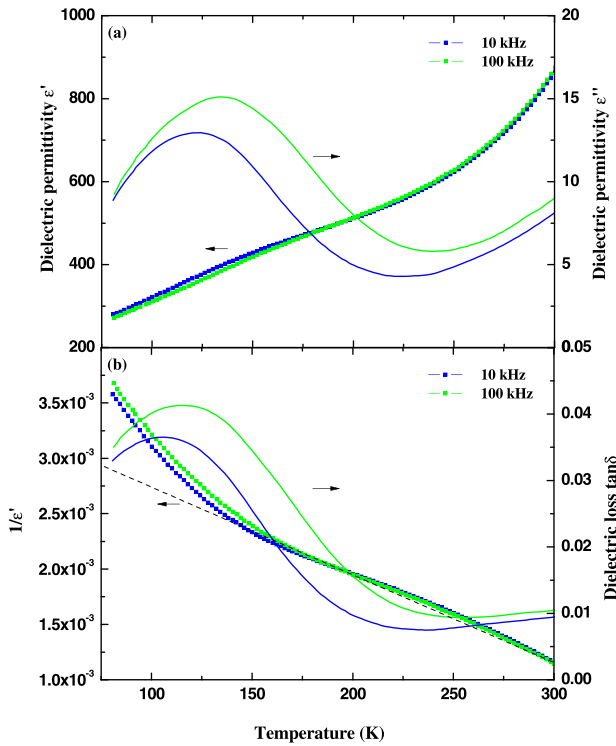


FIG. 4. Temperature dependence of (a) the real and imaginary parts of dielectric permittivity, and (b) the reciprocal of the real part and the dielectric loss of [111] oriented and poled PZN – 6%PT single crystal at various frequencies.

(Fig. 5). A single diffraction peak was observed which confirms that the low temperature phase is in single domain state. The persistence of the dielectric anomaly in this domain-wall-free sample indicates that it cannot be attributed to the motion/relaxation of domain walls.

For better understanding, thermal depolarization current and macroscopic polarization measurements were carried out for [001] (Fig. 6(a)) and [111] (Fig. 6(b)) oriented single crystals. Very weak current signals were observed until about 180 K. Multiple and relatively strong current signals

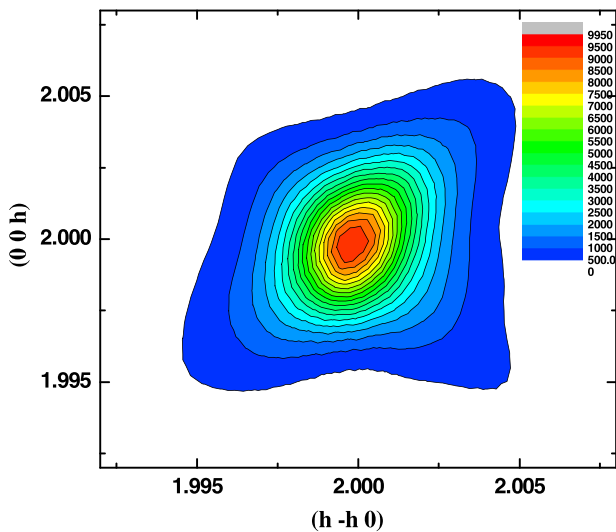


FIG. 5. $\theta - \omega$ mapping in the reciprocal plane perpendicular to the [110] direction carried out around the (222) reflection for [111] oriented and poled PZN – 6%PT single crystal.

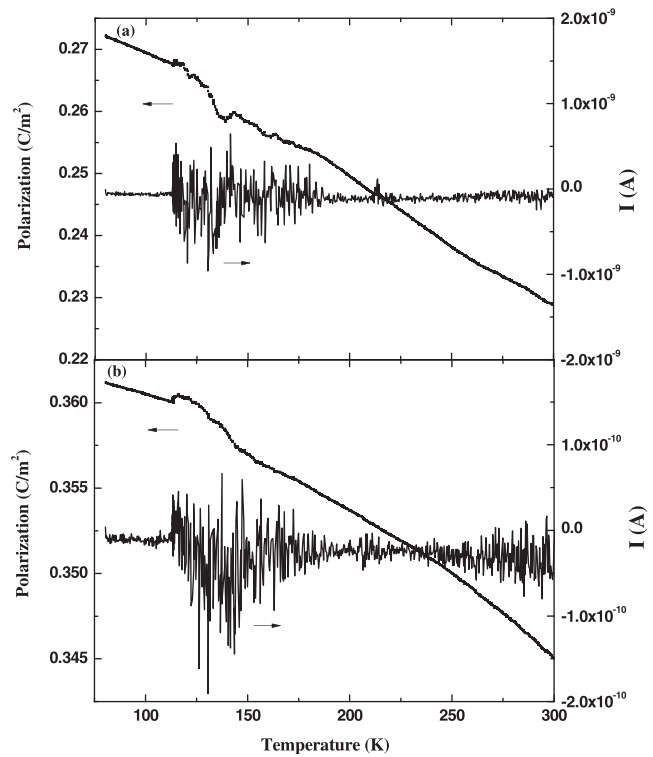


FIG. 6. Temperature dependence of the macroscopic polarization and thermal depolarization current for poled PZN – 6%PT single crystal oriented along (a) [001] and (b) [111] directions.

were detected in the temperature region of 180 – 110 K (in the same range of the dielectric anomaly), followed by a temperature region showing no perceptible current activities until 80 K. These current signals indicate changes in the state of the surface charges arising from changes in local polarization in the material. This behavior is quite clear in the thermal evolution of the macroscopic polarization. On cooling, the polarization grows smoothly until 180 K, where it then shows small fluctuations over from 180 K to 110 K. At lower temperatures, the macroscopic polarization reaches its original value. We shall discuss these results in more detail later.

We also performed mechanical characterizations of our single crystal samples. Fig. 7 shows the temperature

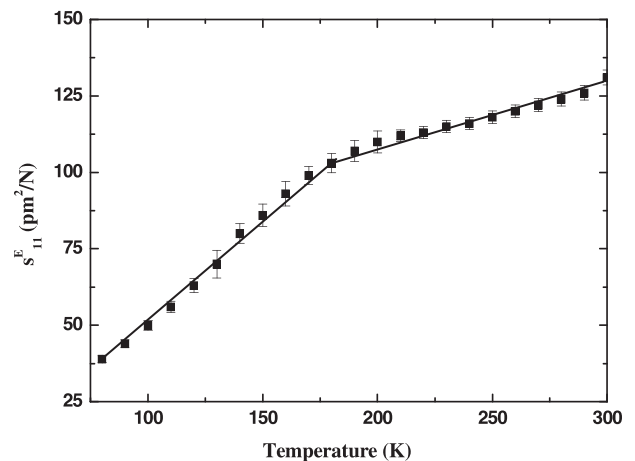


FIG. 7. Temperature dependence of elastic compliance s_{11}^E for [001] oriented PZN – 6%PT single crystal.

dependence of the elastic compliance s_{11}^E for the poled [001] oriented crystal. From higher temperatures, s_{11}^E decreases linearly with temperature on cooling from 300 K, but it exhibits a sharp increase in slope below 180 K, indicating mechanical hardening of the material at low temperature. This behavior is also observed in PZN-4.5%PT (Ref. 14) and the PMN-PT (Ref. 31) system.

The question we raise now is, “What is the physical origin of these observations at low temperature?”

As commented on previously, three models have been proposed in the literature to explain the low temperature dielectric behavior. Our results show clearly that it cannot be associated with a structural phase transition or domain wall motion. The last model points out that structural irregularities (or PNRs) are the main cause of the aforementioned dielectric anomaly. In this situation, it is supposed that the PNRs, which appear a few hundred degrees above the Curie temperature, are embedded and persist within the ferroelectric phases up to a composition of 22% in the case of the PZN- x %PT system.³⁵ The coexistence and the competition of short (PNRs) and long (ferroelectric domain) range orders are evidenced, in several papers,^{8-13,36} from neutron and x-ray diffuse scattering. In our case, a diffuse scattering intensity is observed around the (222) Bragg reflection (Fig. 5) confirming the persistence of the PNRs in the rhombohedral ferroelectric single domain state. Previous works on PZN-4.5%PT (Refs. 37 and 38) and PMN (Ref. 39) have shown that the diffuse scattering intensity consists of both static (elastic) and dynamic (quasielastic) components. On cooling, the elastic component increases while the quasielastic component diminishes and the diffuse scattering intensity becomes completely static between 200 and 50 K.^{37,38} This is the same temperature range in which we have observed the dielectric anomalies, the broadening of the Bragg peaks, the fluctuations in the macroscopic polarization, and the change in slope of the decrease in the elastic compliance.

In the light of the above, the ferroelectric states of the PZN- x %PT (with $0\% \leq x \leq 22\%$) system can be described as polar regions of nanometer scale (PNRs) associated with large dipoles having randomly distributed directions, dispersed within a ferroelectric matrix. At high temperature, the PNRs are largely dynamic, i.e., the local polarizations depend on time and space. On cooling, the PNRs dynamics slow down (some PNRs become static) and at low enough temperature all PNRs freeze, leaving a static local polarization that changes from one PNR to another. On the basis of this simple model, most of the above observations at low temperature can be explained.

Above the temperature of the dielectric anomalies and in the ferroelectric phase, both PNRs and the ferroelectric matrix (ferroelectric domains and domain walls) contribute to the dielectric permittivity. On cooling, the dynamics of PNRs slow down, doing so more rapidly from 200 K to 110 K, which reduces the PNRs ability to polarize in response to an electric field. This explains the change in slope observed in the real part of the dielectric permittivity in the case of poled samples. For unpoled samples, other extrinsic contributions, mainly from domain wall vibration, mask this behavior.

In parallel with this transition to the static state, the stored energy within the medium, through the dynamic of PNRs, will be dissipated. This is the origin of the peaks observed in the imaginary part of the dielectric permittivity and the dielectric loss. Dispersion phenomena and the shift of the temperature of the maximum dielectric loss with frequency are eventually due to a distribution of PNR sizes.

The local polarization of the ferroelectric phase consists of two parts: the polarization from ionic displacements and the polarization of PNRs. Cooling from high temperature, the dynamics of PNRs slows, and some of them become static, which leads to the thermal depolarization current signals observed above 180 K. Between 180 and 110 K, the number of static PNRs increases sharply, consequently the polarization fluctuates (increases or decreases according to whether or not the projection of the polarization of the static PNR is in the same direction as that of the macroscopic polarization). When all PNRs have frozen into a static state, and given their homogeneous distribution, the total polarization of the PNRs becomes zero and the macroscopic polarization reaches its original value.

The transition of the PNRs from the dynamic to the static state creates regions under stress (local strain) within the material,¹⁰ which explains the broadening of Bragg peaks and the decrease in the mechanical compliance.

In conclusion, we have demonstrated in this section that the above mentioned low temperature observations originate from polar nanoregions that lie within micron-sized ferroelectric domains.

B. Temperature dependence of piezoelectric coefficient

The piezoelectric coefficient $d_{31}^{[001]/[100]}$ of [001]-oriented and poled PZN-6%PT single crystal was measured as a function of temperature using the resonance-antiresonance method (Fig. 8). At temperatures below 180 K, the decrease in d_{31} occurs more rapidly on cooling. This reduction of piezoelectric activity cannot be attributed to the quenching of extrinsic contributions, such as domain wall motion, because the domain configuration of the poled state is very stable.

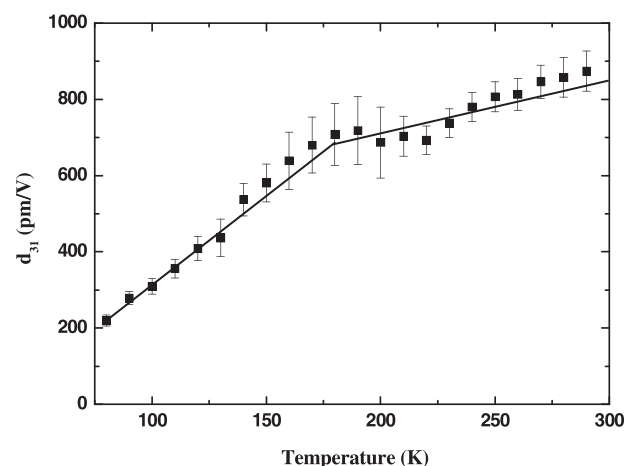


FIG. 8. Temperature dependence of piezoelectric coefficient d_{31} for [001] oriented PZN - 6%PT single crystal.

It is important to note that d_{31} , S_{11}^E , and ε' curves exhibit very similar trends proving that they are governed by the same mechanisms. If we accept that the origin of the dielectric and mechanical anomalies at low temperature is the freezing of PNRs, then we can attribute the observed change in slope on the piezoelectric coefficient to the same phenomenon. This conclusion implies that the PNRs contribute to the ultrahigh piezoelectric response of the PZN- x %PT system, and that their contributions may be the most important part.^{11,14}

IV. SUMMARY

In summary, electromechanical, XRD, and pyroelectric measurements of [001] and [111] oriented PZN-6%PT crystals have been performed from room temperature down to 80 K. Both unpoled and poled samples show a dielectric anomaly at cryogenic temperature. Our results suggest that this behavior originates from the freezing of the dynamics of PNRs at low temperature, giving dielectric evidence of the persistence of these PNRs within the ferroelectric domains. The coexistence of short and long-range polar order and the dynamics of the PNRs can explain also the broadening of the Bragg peaks, the fluctuations in the macroscopic polarization and the change in the rate of decrease of the elastic compliance at cryogenic temperature. Finally, for the [001] direction, it was found that the decrease in the piezoelectric coefficient is more dramatic within the temperature range of the dielectric anomaly. This result provides a direct link between the dynamics of PNRs and the piezoelectric properties of the PZN- x %PT ferroelectric relaxor system.

ACKNOWLEDGMENTS

The first author is grateful to French government and Umm Al-Qura University for financial support.

¹S.-E. Park and T. R. Shrout, *J. Appl. Phys.* **82**, 1804 (1997).

²S.-E. Park and T. R. Shrout, *IEEE Trans. Ultrason., Ferroelectr. Freq. Control* **44**, 1140 (1997).

³H. Fu and R. E. Cohen, *Nature* **403**, 281 (2000).

⁴Z. Kutnjak, J. Petzelt, and R. Blinc, *Nature* **441**, 956 (2006).

⁵A. A. Bokov and Z.-G. Ye, *J. Mater. Sci.* **41**, 31 (2006).

⁶L. E. Cross, *Ferroelectrics* **76**, 241 (1987).

⁷G. Burns and F. H. Dacol, *Phys. Rev. B* **28**, 2527 (1983).

⁸G. Xu, P. M. Gehring, and G. Shirane, *Phys. Rev. B* **72**, 214106 (2005).

⁹G. Xu, P. M. Gehring, and G. Shirane, *Phys. Rev. B* **74**, 104110 (2006).

¹⁰G. Xu, Z. Zhong, Y. Bing, Z.-G. Ye, and G. Shirane, *Nature Mater.* **5**, 134 (2006).

¹¹G. Xu, J. Wen, C. Stock, and P. M. Gehring, *Nature Mater.* **7**, 562 (2008).

¹²J. Wen, G. Xu, C. Stock, and P. M. Gehring, *Appl. Phys. Lett.* **93**, 082901 (2008).

¹³G. Xu, *J. Phys. Soc. Jpn.* **79**, 011011 (2010).

¹⁴S. M. Farnsworth, E. H. Kisi, and M. A. Carpenter, *Phys. Rev. B* **84**, 174124 (2011).

¹⁵M. Matsuura, K. Hirota, P. M. Gehring, Z.-G. Ye, W. Chen, and G. Shirane, *Phys. Rev. B* **74**, 144107 (2006).

¹⁶H. Cao, P. M. Gehring, C. P. Devreugd, J. A. Rodriguez-Rivera, J. Li, and D. Viehland, *Phys. Rev. Lett.* **102**, 127201 (2009).

¹⁷A.-E. Renault, H. Dammak, G. Cabvarin, M. Pham Thi, and P. Gauchrer, *Jpn. J. Appl. Phys., Part 1* **41**, 3846 (2002).

¹⁸S. J. Zhang, L. Lebrun, S. Rhee, R. E. Eitel, C. A. Randall, and T. R. Shrout, *J. Cryst. Growth* **236**, 210 (2002).

¹⁹IEEE Ultrasonics, Ferroelectrics, and Frequency Control Society, The Institute of Electrical and Electronics Engineers, IEEE Standard on Piezoelectricity IEEE, ANSI/IEEE Standard No. 176-1987, 1987.

²⁰Z. Yu, C. Ang, E. Furman, and L. E. Cross, *Appl. Phys. Lett.* **82**, 790 (2003).

²¹P. Bao, F. Yan, Y. Dai, J. Zhu, Y. Wang, and H. Luo, *Appl. Phys. Lett.* **84**, 5317 (2004).

²²S.-E. Park, M. L. Mulvihill, G. Risch, and T. R. Shrout, *Jpn. J. Appl. Phys., Part 1* **36**, 1154 (1997).

²³M. L. Mulvihill, L. E. Cross, W. Cao, and K. Uchino, *J. Am. Ceram. Soc.* **80**, 1462 (1997).

²⁴J. J. Lima-Silva, I. Guedes, J. Mendes Filho, A. P. Ayala, M. H. Lente, J. A. Eiras, and D. Garcia, *Solid State Commun.* **131**, 111 (2004).

²⁵B. K. Singh and B. Kumar, *Mater. Lett.* **63**, 625 (2009).

²⁶X. Wan, R. K. Zheng, H. L. W. Chan, C. L. Choy, X. Zhao, and H. Luo, *J. Appl. Phys.* **96**, 6574 (2004).

²⁷S. Priya, D. Viehland, and K. Uchino, *Appl. Phys. Lett.* **80**, 4217 (2002).

²⁸M. Thiercelin, H. Dammak, and M. Pham Thi, in International Symposium on the Applications of Ferroelectrics ISAF, 2010.

²⁹Z. Li, Z. Xu, Z. Xi, L. Cao, and X. Yao, *J. Electroceram.* **21**, 279 (2008).

³⁰F. Wang, S. W. Or, X. Zhao, and H. Luo, *J. Phys. D: Appl. Phys.* **42**, 182001 (2009).

³¹F. Martin, H. J. M. ter Brake, L. Lebrun, S. Zhang, and T. Shrout, *J. Appl. Phys.* **111**, 104108 (2012).

³²D. La-Orauttapong, B. Noheda, Z.-G. Ye, P. M. Gehring, J. Toulouse, D. E. Cox, and G. Shirane, *Phys. Rev. B* **65**, 144101 (2002).

³³D. E. Cox, B. Noheda, G. Shirane, Y. Uesu, K. Fujishiro, and Y. Yamada, *Appl. Phys. Lett.* **79**, 400 (2001).

³⁴G. Xu, Z. Zhong, Y. Bing, Z.-G. Ye, C. Stock, and G. Shirane, *Phys. Rev. B* **70**, 064107 (2004).

³⁵M. Tachibana, K. Sasame, H. Kawaji, T. Atake, and E. Takayama-Muromachi, *Phys. Rev. B* **80**, 094115 (2009).

³⁶I.-K. Jeong, *Phys. Rev. B* **79**, 052101 (2009).

³⁷Z. Xu, J. Wen, G. Xu, C. Stock, J. S. Gardner, and P. M. Gehring, *Phys. Rev. B* **82**, 134124 (2010).

³⁸Z. Xu, J. Wen, E. Mamontov, C. Stock, P. M. Gehring, and G. Xu, *Phys. Rev. B* **86**, 144106 (2012).

³⁹C. Stock, L. Van Eijck, P. Fouquet, M. Maccarini, P. M. Gehring, G. Xu, H. Luo, X. Zhao, J.-F. Li, and D. Viehland, *Phys. Rev. B* **81**, 144127 (2010).